Robust Gust Load Alleviation for a Flexible Aircraft

Nabil Aouf, Benoit Boulet
Centre for Intelligent Machines
McGill University
3480 University Street, Montréal, Québec,
Canada H3A 2A7
Tel: (514) 398-1478, Fax: (514) 398-4470
E-mail: aouf@cim.mcgill.ca, boulet@cim.mcgill.ca,

Ruxandra Botez
Département de Génie de la production automatisée
Ecole de technologie supérieure
1100 Notre-Dame Street West, Montréal, Québec,
Canada H3C 1K3
Tel: (514) 396-8560, Fax: (514) 396-8595
E-mail: ruxandra@gpa.etsmtl.ca

Abstract

An $\mathcal{H}_\infty$ controller design is presented to establish a nominal performance baseline for the vertical acceleration control of a B-52 aircraft model with flexibility. μ-synthesis and analysis is used to study the robust performance of the aircraft taking into account specific input and output multiplicative uncertainty models. The aircraft is assumed to be subjected to severe wind gusts causing undesirable vertical motion. We use the Dryden gust power spectral density model to guide the performance specifications and control designs, as well as for time-domain simulations. Motivation for the use of an $\mathcal{H}_\infty$ nominal performance baseline specification is given in terms of a new interpretation of the Dryden model. The $\mathcal{H}_\infty$ optimal controller is shown to reduce dramatically the effect of wind gust on the aircraft vertical acceleration. Robust performance is achieved with a μ-synthesis controller design using a *D-K* iteration procedure.

I- INTRODUCTION

Gust load alleviation (GLA) systems can be used to reduce the effects of wind gusts on vertical acceleration of aircraft. Their purpose is to reduce airframe loads and improve passenger comfort. In this paper, the longitudinal dynamics of the B-52 bomber are studied [6]. The dynamic model of the aircraft includes structural flexibility. Such a model is more realistic than a rigid-body model, but it can also make feedback control design for gust load alleviation more challenging.

We present $\mathcal{H}_\infty$ and μ controller designs for a model of the B-52 aircraft with flexible modes. The gust is generated with the Dryden power spectral density model. This kind of model lends itself well to frequency-domain performance specifications in the form weighting functions. The $\mathcal{H}_\infty$ and μ controllers are shown to meet the desired nominal performance and the robust performance specifications with reasonably small control surface deflection angles.

Previous research on GLA control systems reported in [2], [5], [7] take approaches different to ours, notably LQG and $\mathcal{H}_\infty$ for a rigid-body aircraft .

II- GUST MODEL

Two classical analytical representations for the power spectral density (PSD) functions of atmospheric turbulence were given by Von Karman and Dryden [6]. As the Dryden PSD function has a simpler form than Von Karman's we chose to use the former. It can be written as:

$$\Phi_w(\omega) = \frac{\sigma_w^2 L_w \left[1 + 3\left(\frac{L_w \omega}{U_0}\right)^2\right]}{\pi U_0 \left[1 + \left(\frac{L_w \omega}{U_0}\right)^2\right]^2} \qquad (1)$$

where:
σ_w is the RMS vertical gust velocity (*m/s*),
L_w is the scale of turbulence (*m*), and
U_o is the aircraft trim velocity (*m/s*).

The scale length L_w is dependent on the aircraft's height h when atmospheric turbulence is encountered, as follows:
At h >580 m (1750 ft), L_w = 580 m,
At h < 580 m, L_w = h m.
For thunderstorms, at any height:
L_w = 580 m (1750 ft), σ_w = 7 m/s (21 ft/s).

Gust signals have to be generated with the required intensity, scale lengths and PSD functions for some given flight velocity and height. In order to generate these gust signals, a noise source with PSD function $\Phi_n(\omega) = 1$ in the frequency band of interest is used to provide the input signal to a linear filter $G_w(s)$ chosen such that the squared magnitude of its frequency response is the PSD function $\Phi_w(\omega)$. The gust generator setup is as follows:

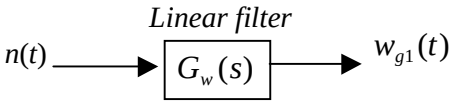

Fig. 1: Gust signal generator

where $n(t) \sim N(0,1)$ is a Gaussian white noise process of unit intensity and zero mean, and $w_{g1}(t)$ is the random continuous vertical gust, so that, formally, $w_{g1} = G_w n$. The PSD of the output signal is related to the PSD of the input signal as follows:

$$\Phi_w(\omega) = |G_w(j\omega)|^2 \quad \Phi_N(\omega) = |G_w(j\omega)|^2 \quad (2)$$

An expression for the Dryden filter can be found through spectral factorization of $\Phi_w(\omega)$, which yields

$$G_w(s) = \sqrt{\frac{3U_0\sigma^2{}_w}{\pi L_w}} \frac{\frac{U_0}{\sqrt{3}L_w} + s}{\left[\frac{U_0}{L_w} + s\right]^2} \qquad (3)$$

A proposed alternative use of the Dryden model is to consider the noise n to be any deterministic finite-energy signal in $\mathcal{N} := \{n \in \mathcal{L}_2[0,\infty) : \|n\|_2 \le 1\}$. The gust signal lives in $\mathcal{W} := \{G_w n : n \in \mathcal{N}\} \subset \mathcal{L}_2[0,\infty)$ and its energy is bounded by $\|w_g\|_2 \le \|G_w\|_\infty = \frac{9\sqrt{2}\sigma_w}{10}\sqrt{\frac{L_w}{\pi U_0}}$. Furthermore, such signals taper off at infinity in the time domain. Hence, they may be more representative of real wind gusts acting on an aircraft passing through a turbulence. Although the stochastic nature of the signal is lost, the resulting set of bounded-energy gust signals can be used for a worst-case $\mathcal{H}_\infty$ design, which is desirable in a safety-critical application such as GLA.

III- FLEXIBLE AIRCRAFT MODEL

The short-period approximation for the rigid-body motion of the B-52 aircraft is considered. The aircraft's rigid-body dynamics equations are augmented by adding to the state variables a set of generalized coordinates associated with the normal bending modes. Structural displacement was considered small compared to the whole aircraft structure. The j^{th} flexible mode is represented by the following second-order linear constant-coefficient differential equation in terms of its modal coordinate η_j:

$$\ddot{\eta}_j + 2\zeta_j\omega_j\dot{\eta}_j + \omega_j{}^2\eta_j = \rho_j\phi_j \quad (4)$$

where ς_j, ω_j, ρ_j are the damping ratio, frequency and gain of the j^{th} flexible mode, and ϕ_j is its corresponding generalized force. Thus, the rigid aircraft dynamics may be augmented with pairs of first-order equations corresponding to each flexible mode considered. Five structural flexible modes were considered significant and were kept in the longitudinal dynamic model of the B-52 aircraft [5].

The control inputs for the longitudinal motion are the deflection angles (in radians) of the elevator δ_{el} and the horizontal canard δ_{hc}. The longitudinal dynamics of the flexible aircraft in terms of the state variable representation is:

$$\dot{x} = Ax + Bu + B_g w_g \quad (5)$$
$$y = Cx + Du$$

where $x \in \mathbb{R}^{12}$ is the state vector,
$x^T =$
$[\alpha \;\; q \;\; \eta_1 \;\; \dot{\eta}_1 \;\; \eta_5 \;\; \dot{\eta}_5 \;\; \eta_7 \;\; \dot{\eta}_7 \;\; \eta_8 \;\; \dot{\eta}_8 \;\; \eta_{12} \;\; \dot{\eta}_{12}]$
$u \in \mathbb{R}^2$ is the control vector, $u = [\delta_{el} \;\; \delta_{hc}]^T$ (radians), $y \in \mathbb{R}$ is the vertical acceleration (g), $w_g \in \mathbb{R}^3$ is the vertical gust velocity at three stations (m/s) , $\alpha \in \mathbb{R}$ is the angle of attack (radians) and $q \in \mathbb{R}$ is the pitch rate (radians/s).

The form of the *A* matrix in state-space equation (5) shows the couplings between the aircraft's flexible structure and rigid-body dynamics:

$$A = \begin{bmatrix} A_{rr} & A_{ra} \\ A_{ar} & A_{aa} \end{bmatrix} \qquad (6)$$

where A_{rr} are the rigid-body terms, A_{ra} the rigid/aeroelastic terms, A_{ar} the aeroelastic/rigid terms, and A_{aa} the structural flexibility terms. The eigenvalues of A corresponding to the rigid-body mode are $\lambda_{1,2} = -1.803 \pm j2.617$. The five flexible modes are listed in Table 1 below.

Table 1: flexible modes

	1	2	3	4	5
ω_i (rd/s)	7.60	15.22	19.73	20.24	38.29
ς_i	0.393	0.056	0.011	0.067	0.023

Input terms associated with the effects of wind gust acting at three different body stations are also included in (5). They appear as three different gust signals w_{g1}, w_{g2}, and w_{g3} acting in the longitudinal dynamic equations. Thus, the gust vector is defined as $w_g=[w_{g1} \;\; w_{g2} \;\; w_{g3}]^T$.

The second and third gust signals w_{g2} and w_{g3} are time-delayed versions of w_{g1}. The second gust is delayed by a time $\tau_1 = U_0/x_1 = 0.06$ s, where x_1 is the distance from the first body station, which encounters the gust first. The third input is delayed by time $\tau_2 = U_0/x_2 = 0.145$ s. First-order lags are used to model the delays. The formal generation of the gust vector is shown in Figure 2.

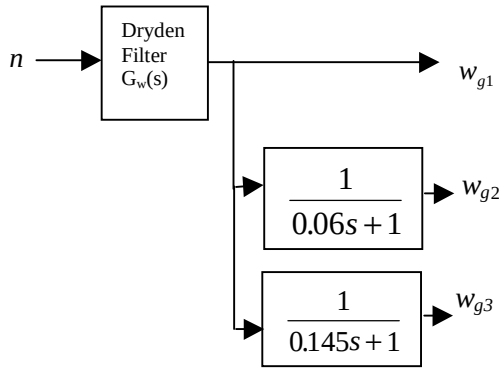

Fig. 2: Gust signals at three body stations

IV- $\mathcal{H}_\infty$-OPTIMAL CONTROL

A- Problem Setup

A block diagram of the closed-loop gust alleviation design problem with weighting functions is shown in Figure 3 below:

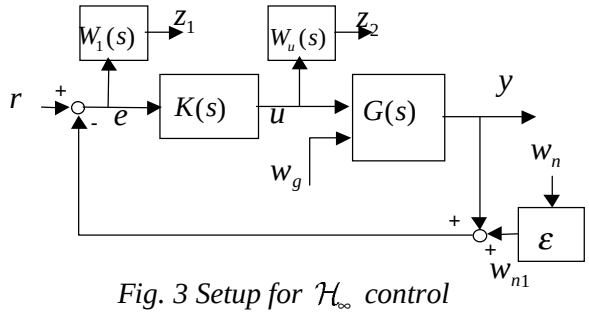

Fig. 3 Setup for $\mathcal{H}_\infty$ control

where $w_g \in \mathbb{R}^3$ is the gust disturbance, $w_{n1} \in \mathbb{R}$ is an acceleration measurement noise, $r = 0$ is the vertical acceleration setpoint, $z_1 \in \mathbb{R}$ is the weighted measured error, and $z_2 \in \mathbb{R}^2$ is the weighted controller output. The plant transfer matrix $G(s)$ mapping $[u \; w_g{}^T]^T$ to y is given by

$$G(s) = \left[\begin{array}{c|c} A & [B \; B_g] \\ \hline C & [D \; 0] \end{array}\right]. \qquad (7)$$

The signal w_{n1} is a small disturbance that has a role to play in regularizing the $\mathcal{H}_\infty$ design problem. It can also be seen as a real measurement noise. Its amplitude is specified by

$\varepsilon = 10^{-4}$ as w_n is assumed to have a maximum amplitude of 1. For convenience, we will use the notation $T_{xy} := x \mapsto y$ for closed-loop transfer matrices mapping signal x to signal y.

B- Weighting Functions for Nominal Performance

Choosing $\sigma_w = 7m/s, L_w = 580m$ in the Dryden model, we obtain a gust that has most of its power concentrated in the frequency band $[0.1, 6]$ Hz. The specification is that our controller has to be able to regulate the vertical acceleration in this interval with an amplitude attenuation of at least 500 (-54 dB).

The closed-loop vertical acceleration of the aircraft can be written in terms of the gust vector w_g and the disturbance w_n as follows:

$$y = T_{w_g y} w_g + T_{w_n y} w_n, \qquad (8)$$

where $T_{w_g y}$ and $T_{w_n y}$ are the transfer matrices mapping w_g and w_n to y respectively. Thus, the controller has to minimize $\left\| T_{w_g y}(j\omega) \right\|$ and $\left\| T_{w_n y}(j\omega) \right\|$ over $[0.1, 6]$ Hz. The gust alleviation performance specification on $\left\| T_{w_g y}(j\omega) \right\|$ can be enforced through the use of a weighting function W_1 of amplitude at least 500 over $[0.1, 6]$ Hz, as long as we get $\left\| W_1 T_{w_g y} \right\|_\infty < 1$ with the controller K, which implies

$$\left\| T_{w_g y}(j\omega) \right\| < \left| W_1(j\omega) \right|^{-1}. \qquad (9)$$

The weighting function is

$$W_1(s) = \frac{k_1}{a_0 s + 1} \qquad (10)$$

with $k_1 = 500$, $a_0 = 0.05$. A plot of $\left| W_1(j\omega) \right|^{-1}$ is shown in Figure 5.

The controller outputs consist of deflection angles (in radians) of the aircraft's elevators and horizontal canards. In order to make sure that these angles will remain within acceptable limits, we took the output of the controller u as one of the controlled variable z_2. Define the input vector $w := [w_g{}^T \; w_n]^T$. The use of a suitable weighting function W_u on u such that $\left\| W_u T_{wu} \right\|_\infty < 1$ in closed loop minimizes actuator travel while meeting the other performance spec. The weighting function W_u is a diagonal transfer matrix $\begin{bmatrix} W_{u1} & 0 \\ 0 & W_{u2} \end{bmatrix}$ so that the above $\mathcal{H}_\infty$-norm condition implies

$$\left\| T_{wu1}(j\omega) \right\| < \left| W_{u1}(j\omega) \right|^{-1} \qquad (11)$$

and

$$\left\| T_{wu2}(j\omega) \right\| < \left| W_{u2}(j\omega) \right|^{-1}, \qquad (12)$$

where $T_{wu} = \begin{bmatrix} T_{wu1} \\ T_{wu2} \end{bmatrix}$. In our study, we tried two different types of control weighting functions. The first type is composed of two first-order biproper filters

$$W_u^1(s) = \begin{bmatrix} \dfrac{s + \omega_{c1}/l_{u1}}{\varepsilon_1 s + \omega_{c1}} & 0 \\ 0 & \dfrac{s + \omega_{c2}/l_{u2}}{\varepsilon_2 s + \omega_{c2}} \end{bmatrix} \qquad (13)$$

where $\varepsilon_1, \varepsilon_2$ are very small. The parameters l_{u1} and l_{u2} represent the maximum controller gains at frequencies below the cutoff frequencies ω_{c1} and ω_{c2}. The second type of control weighting function that we tried is constant:

$$W_u^2 = \begin{bmatrix} k_{u1} & 0 \\ 0 & k_{u2} \end{bmatrix}. \qquad (14)$$

Here $1/k_{u1}$ and $1/k_{u2}$ represent the maximum controller gains at all frequencies in closed loop. For both types of weighting functions, we took $k_{u1}{}^{-1} = l_{u1} = 0.2$, $k_{u2}{}^{-1} = l_{u2} = 0.5$ and $\varepsilon_1 = \varepsilon_2 = 0.0001$.

The weighting function $W_u^1(s)$ gives us more degrees of freedom to constrain the control signals in order to satisfy physical actuator saturation and bandwidth constraints. In our case study, the filter cutoff frequencies were selected

as $\omega_{c1} = 12, \omega_{c2} = 13$ rd/s. However, it finally proved preferable to use the constant weighting matrix W_u^2 for our application, since it did not increase the order of the generalized plant model $P(s)$ by 2 like $W_u^1(s)$ would, (and hence the resulting $\mathcal{H}_\infty$ controller would have a lower order). Moreover, the resulting closed-loop transfer functions still satisfied inequalities (11) and (12) with $W_u^1(s)$. Figures 6 and 7 show the magnitude of W_u with both forms.

C- $\mathcal{H}_\infty$ Controller

The GLA problem of Figure 3 can be recast into the standard $\mathcal{H}_\infty$-optimal control problem [4] of Figure 4 below.

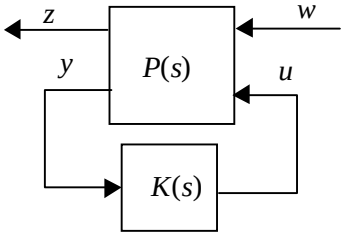

Fig. 4: Standard setup for $\mathcal{H}_\infty$ control

The nominal generalized plant model

$$P(s) = \begin{bmatrix} P_{11}(s) & P_{12}(s) \\ P_{21}(s) & P_{22}(s) \end{bmatrix} \qquad (15)$$

has a minimal state-space realization

$$\begin{aligned} \dot{x} &= A_P x + B_{P1} w + B_{P2} u \\ z &= C_{P1} x + D_{P11} w + D_{P12} u \\ y &= C_{P2} x + D_{P21} w + D_{P22} u \end{aligned} \qquad (16)$$

which combines the aircraft model and realizations of the weighting functions. The vector of exogenous signals is $w = [w_g^{\ T} \ w_n]^T$ and the signals to be minimized are collected in $z := [y \ u^T]^T$.

As gusts act over a relatively short period of time, they can be considered as signals with finite energy. Such signals can have spectral contents similar to the *PSD* of stochastic Dryden gust signals by using $G_w(s)$ as a filter. This remark provides motivation for $\mathcal{H}_\infty$ GLA control design as

$$\begin{aligned} &\min_{K\in\mathcal{S}} \max_{w\in\mathcal{W}} \|T_{wz} w\|_2 = \min_{K\in\mathcal{S}} \max_{n\in\mathcal{N}} \|T_{wz} G_w n\|_2 \\ &= \min_{K\in\mathcal{S}} \|T_{wz} G_w\|_\infty = \min_{K\in\mathcal{S}} \sup_{\omega\in\mathbb{R}} \|T_{wz}(j\omega) G_w(j\omega)\| \end{aligned} \qquad (17)$$

where $\mathcal{S}$ is the set of all finite-dimensional, causal linear time-invariant stabilizing controllers. Note that we chose to use the performance weighting function $W_1(s)$ instead of $G_w(s)$ in our design, but $|W_1(j\omega)| > |G_w(j\omega)|$ at all frequencies, which leads to better performance.

The overall objective in this $\mathcal{H}_\infty$-optimal controller design was to minimize $\|T_{wz}\|_\infty$ over the set $\mathcal{S}$, in order to get $\|T_{wz}\|_\infty < 1$. This would guarantee that the performance specification is satisfied on the nominal model. Following [4], an $\mathcal{H}_\infty$ controller $K(s)$ of order 13 was designed using the Matlab μ-Synthesis and Analysis Toolbox [1] that achieved a norm of $\|T_{wz}\|_\infty = 0.68$. Figure 5 shows that our $\mathcal{H}_\infty$ controller meets the gust alleviation performance specification given above. We can see that the maximum singular value of $T_{w_g y}$ is well below 10^{-4} over $2\pi[0.1, 6]$ rd / s.

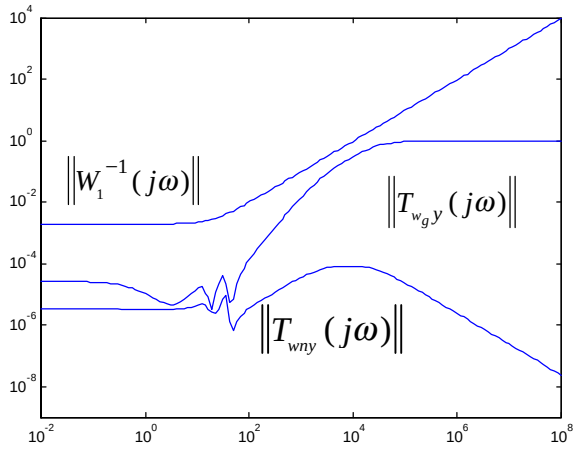

Fig. 5: Achieved performance

The norms (maximum singular values) of the frequency responses of T_{wu1} and T_{wu2} shown in Figures 6 and 7 satisfy the constraints of (11) and (12) for both control weighting functions as mentioned above.

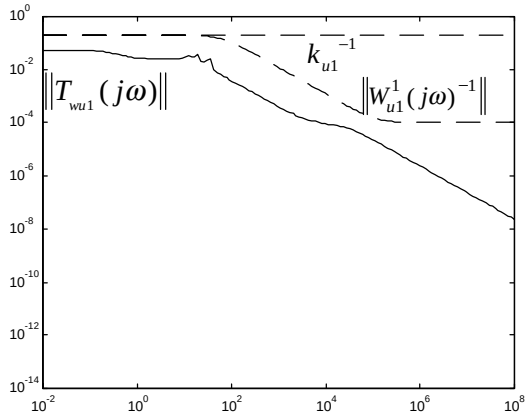

Fig. 6: Constraint on elevator angle

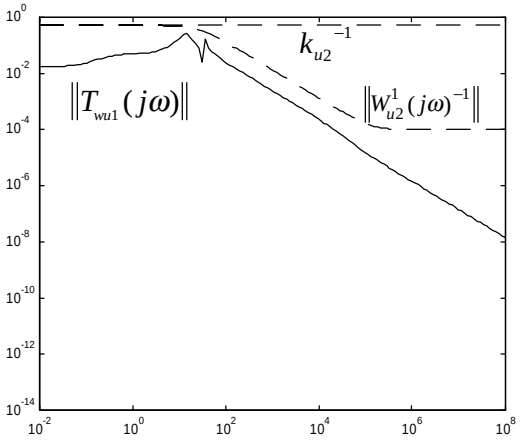

Fig. 7: Constraint on horizontal canard angle

V- μ – CONTROLLER

The $\mathcal{H}_\infty$ controller design of the previous section provides nominal performance. That is, performance is guaranteed only if the model represents the aircraft's dynamics perfectly, which is clearly too optimistic. In this section, uncertainty in the frequency responses of the actuators and sensors is taken into account in the model and the controller design. Note that this uncertainty may also include variations in the aerodynamics of the control surfaces which may be caused by changes in altitude and velocity of the aircraft. As shown in Figure 8, we include two complex multiplicative uncertainty blocks in the model: $\Delta_u := \mathrm{diag}\{\Delta_{u1}, \Delta_{u2}\}$, $\Delta_{u1}, \Delta_{u2} \in \mathbb{C}$ and $\Delta_y \in \mathbb{C}$. These perturbations represent the uncertainty in the frequency responses of the actuators and the sensor, respectively. The corresponding weighting functions are

$$W_{uncu} = \begin{pmatrix} \dfrac{0.75s+50}{s+400} & 0 \\ 0 & \dfrac{0.75s+22.5}{s+400} \end{pmatrix}, \quad (18)$$

$$W_{uncy} = \frac{0.15s+30}{s+100} \quad (19)$$

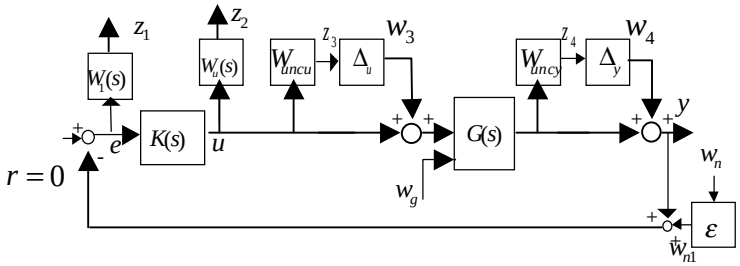

Fig. 8: Setup for robust control design

This design can be recast into the general μ – synthesis setup as given by Figure 9. Define the complex structured uncertainty set

$$\Omega := \{\Delta = \mathrm{blockdiag}\{\Delta_{u1}, \Delta_{u2}, \Delta_y\} : \Delta_{u1}, \Delta_{u2}, \Delta_y \in \mathbb{C}\} \subset \mathbb{C}^{3\times 3} \quad (20)$$

and the augmented structured uncertainty set

$$\Gamma := \{\Delta_s = \mathrm{blockdiag}\{\Delta, \Delta_p\} : \Delta \in \Omega, \Delta_p \in \mathbb{C}^{4\times 3}\} \subset \mathbb{C}^{7\times 6} \quad (21)$$

where $\Delta_p \in \mathbb{C}^{4\times 3}$ is a fictitious uncertainty linking the exogenous inputs $\begin{bmatrix} w_g & w_n \end{bmatrix}^T$ to the output variables $\begin{bmatrix} z_1 & z_2 \end{bmatrix}^T$. This fictitious perturbation is included to transform a robust performance design problem into an equivalent robust stability problem, which is easier to solve [1]. The inputs and outputs of the structured uncertainty $\Delta_s(s) \in \mathcal{H}_\infty$, $\Delta_s(j\omega) \in \Gamma$ in Figure 9 are, respectively, the vectors

$z_s = \begin{bmatrix} z_3^T & z_4 & z_1 & z_2^T \end{bmatrix}^T \in \mathbb{R}^6$ and $w_s = \begin{bmatrix} w_3^T & w_4 & w_g^T & w_n \end{bmatrix}^T \in \mathbb{R}^7$.

The structured singular value μ_Γ of a complex matrix $M \in \mathbb{C}^{6\times 7}$ is defined with respect to the structured uncertainty set Γ as follows:

$$\mu_\Gamma(M) := \min\left\{\|\Delta\| : \Delta \in \Gamma, \det(I - M\Delta) = 0\right\}^{-1} \quad (22)$$

unless no such perturbation exists, in which case $\mu_\Gamma(M) = 0$.

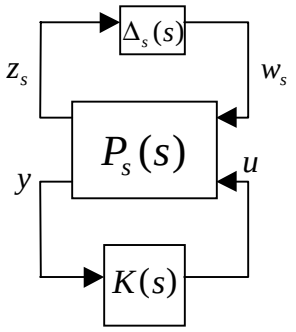

Fig. 9: Standard setup for μ_Γ design

A robust controller design based on μ_Γ is less conservative than a robust $\mathcal{H}_\infty$ design (not to be confused with our $\mathcal{H}_\infty$ controller of the previous section which is optimal for the nominal model, but was not designed to be robust to model uncertainty). This is because the structured uncertainty Δ_s is taken into account as a full block of uncertainty in a typical robust $\mathcal{H}_\infty$ design.

A $\mu-$synthesis consists of finding the optimal controller that minimizes the peak value of $\mu_\Gamma[T_{wz}(j\omega)]$ over all frequencies. That is,

$$\min_{K(s)\in S} \sup_{\omega\in\mathbb{R}} \mu_\Gamma[T_{wz}(j\omega)]. \quad (23)$$

Compare this with the optimization problem for the $\mathcal{H}_\infty$ controller design in (17). The main benefit offered by $\mu-$synthesis is robust performance. That is, according to the Main Loop Theorem [1], if a controller achieves $\sup_{\omega\in\mathbb{R}} \mu_\Gamma[T_{w_s z_s}(j\omega)] < 1$, then stability and the performance specification $\|T_{wz}\|_\infty < 1$ hold for all $\Delta(s) \in \mathcal{H}_\infty, \|\Delta\|_\infty \le 1, \Delta(j\omega) \in \Omega$.

It is well known that no algorithm is yet available to compute $\mu_\Gamma(M)$ in the general case (including our case). Thus, the optimization problem (23) cannot be solved directly. However, the so-called *D-K iteration* algorithm [1] has been proposed to minimize an upper bound for μ_Γ. The D-K iteration is an attempt to solve

$$\min_{K\in S, D_l, D_r} \left\| D_l T_{w_s z_s} D_r^{-1} \right\|_\infty \quad (24)$$

where the so-called left and right D-scales $D_l(s), D_r(s) \in \mathcal{H}_\infty$ are minimum-phase and have frequency responses of the form

$$D_l(j\omega) \in \mathcal{D}_l := \left\{\text{diag}\{d_1, d_2, d_3, I_4\} : d_1, d_2, d_3 \in \mathbb{R}_+\right\}$$

$$D_r(j\omega) \in \mathcal{D}_r := \left\{\text{diag}\{d_1, d_2, d_3, I_3\} : d_1, d_2, d_3 \in \mathbb{R}_+\right\}$$

This algorithm involves an iterative sequence of minimizations over $K(s) \in S$ (holding the D-scales fixed) using the $\mathcal{H}_\infty$ technique, then over the D-scales (holding $K(s)$ fixed).

VI- SIMULATION RESULTS

In this section, we use the Dryden model with parameters $\sigma_w = 7\, m/s$, $L_w = 580m$ to generate severe wind gusts for simulation purposes. Figure 10 shows the gust vector used in our simulations.

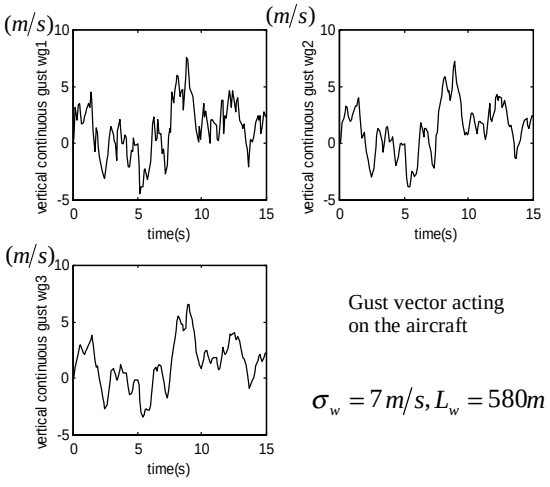

Fig.10: Gust signals for simulation

Figure 11 shows a magnitude plot of the frequency response of the Dryden filter for simulation. We can see that the performance specification enforced by the weighting function should result in efficient GLA.

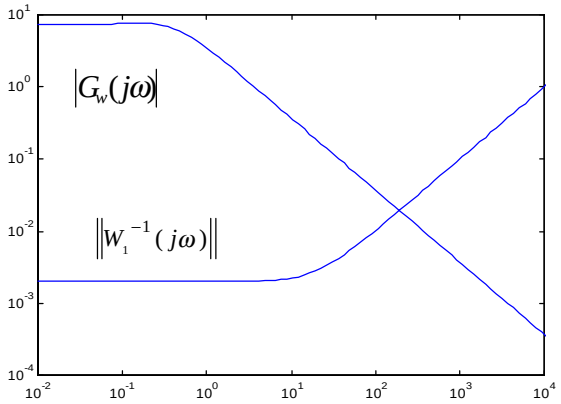

Fig. 11: Dryden filter and performance weighting

Time-domain simulations were conducted and results are presented below. The results confirm that the $\mathcal{H}_\infty$ controller can dramatically reduce the effect of wind gusts on the vertical acceleration of the aircraft for the nominal model comparing to the results of different $\mathcal{H}_2$ (LQG) controllers [2],[3].

The goal of the simulation with the nominal model (without uncertainties) is to show that our $\mathcal{H}_\infty$ controller can deal with strong turbulence without exciting the flexible modes or generating large control angles that would saturate the control surfaces. Figure 12 and 13 show respectively the effect of the gust $w_g = [w_{g1} w_{g2} w_{g3}]^T$ on the B-52 aircraft, without using a feedback controller (Fig. 12), and with the $\mathcal{H}_\infty$ controller (Fig. 13).

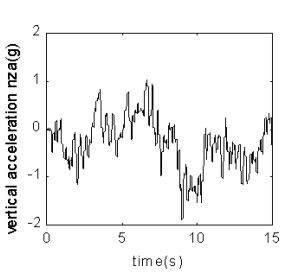

Fig. 12: Open-loop

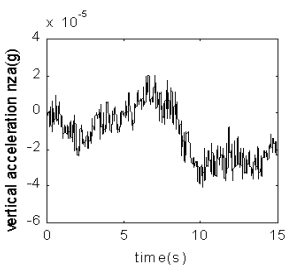

Fig. 13: $\mathcal{H}_\infty$ control

These plots show a dramatic improvement in flight comfort. Figures 17 and 18 show the control angles. Notice that the angle swings of the elevator and the horizontal canard control surfaces were reasonable.

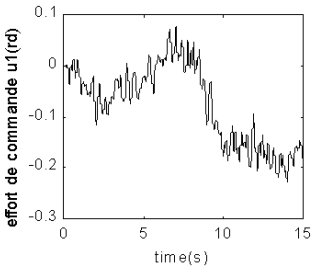

Fig. 14: Elevator

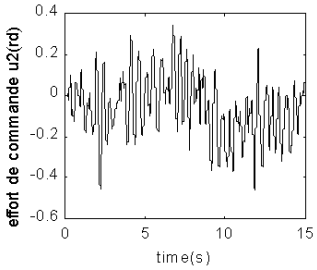

Fig. 15: Horizontal canard

Figure 16 below shows the magnitude of the weighting functions

$$W_{uncu}(s) = \begin{bmatrix} W_{uncu1}(s) & 0 \\ 0 & W_{uncu2}(s) \end{bmatrix}, \quad W_{uncy}(s).$$

These weighting functions specify the amount of uncertainty in the actuators and the sensor, respectively. We specified nearly 20% of uncertainty at low frequencies for the first actuator (elevator) and around 8% of uncertainty for the second actuator (horizontal canard). For the sensor we assumed an uncertainty of 3.5% at low frequencies. These uncertainties grow with frequency until they reach a constant level at high frequencies.

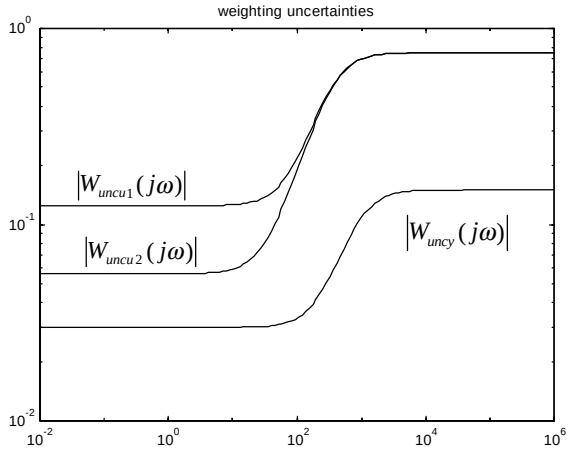

Fig. 16: Norm bounds for uncertainties

Our μ controller obtained using a D-K iteration reached the robust performance specified. Figure 17 shows the $\mu-$bounds for the controller

obtained in the second D-K iteration. The maximum of the upper bound for μ across frequencies is equal to 0.792, and therefore robust performance was achieved.

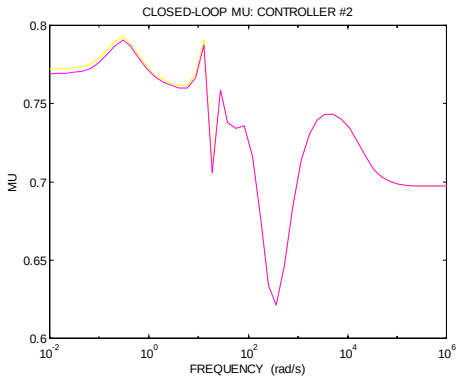

Fig. 17: Upper and lower bounds on μ for μ design

An $\mathcal{H}_\infty$ controller designed for the model with uncertainties led to an maximum norm of the frequency response of the closed-loop system equal to 15.35. This is too high and hence unacceptable from a robust performance point of view. A $\mu-$analysis was done for the $\mathcal{H}_\infty$ controller and the results are shown in Figure 18. It is seen that the maximum of μ obtained with the $\mathcal{H}_\infty$ controller is equal to 3.1. This value being much larger than one confirms the loss of robust performance.

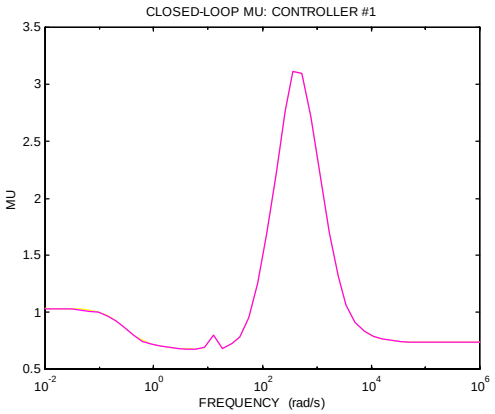

Fig. 18 Upper and lower bounds on μ , $\mathcal{H}_\infty$ design

This was expected because the $\mathcal{H}_\infty$ design is unable to take into account the structure of the uncertainty as opposed to the $\mu-$design.

VII- CONCLUSION

We presented a GLA $\mathcal{H}_\infty$-optimal controller design for a B-52 aircraft model with flexible modes. The gust was generated with a Dryden power spectral density model. This kind of model lends itself well to frequency-domain performance specifications in the form of weighting functions. The $\mathcal{H}_\infty$ controller was shown to meet the desired performance specification with reasonably small control surface deflection angles. A μ design was then developed for a perturbed model including multiplicative uncertainties in the actuators and the sensor. The μ controller reached the robust performance level specified. We also compared an $\mathcal{H}_\infty$ controller design for this uncertain model with the μ design. We pointed out the loss of robust performance of the $\mathcal{H}_\infty$ design compared to the μ design. Future research will focus on the issues related to uncertain modal parameters and different flight envelopes.

VIII- REFERENCES

[1] Balas, G.J., Doyle, J.C., Glover, K., Packard, A., Smith, R., 1995 μ-Analysis and synthesis toolbox MUSYN Inc, and the MathWorks, Inc.

[2] Botez, R.M., Boustani, I. and Vayani, N., "Optimal control laws for gust load alleviation", 1999, Proceedings of the CASI 46th Annual Conference, pp. 649-655, May 3-5, Montréal, Québec, Canada.

[3]- N.Aouf, B.Boulet, R.Botez. $\mathcal{H}_2$ and $\mathcal{H}_\infty$ optimal gust load alleviation for a flexible aircraft. To appear in *Proc. of 2000 American Control Conference,* Chicago.

[4] Doyle, J.C., Glover, K., Khargonekar, P., Francis, B., 1988. State space solutions to standard $\mathcal{H}_2$ and $\mathcal{H}_\infty$ control problems. IEEE Trans. Automatic Control AC-24(8), 731-747.

[5] Mclean, D, 1978, Gust load alleviation control systems for aircraft. Proc. IEE, Vol.125, No.7, July, pp. 675-685.

[6] Mclean, D, 1990. Automatic flight control systems. Prentice Hall International, Series in Systems and Control engineering.

[7] Niewoehner, R.J., and Kaminar, I.I., 1996 Design of an autoland controller for an F-14 Aircraft using $\mathcal{H}_\infty$ synthesis. *Journal of Guidance, Control, and Dynamics*, Vol. 19, No 3, May, pp. 656-663.